Hyperspectral Image based Crop Classification enabled by Machine Learning

Vaishnavi S. Ghatge, Vaishnavi S. Alur, Shivani L. Hadapad, Snehal S. Patil, GujanattiRudrappa[*], Arun S. Tigadi, Sadanand B. Kulkarni

Department of Electronics and Communication Engineering, KLE Technological University-MSSCET, Belagavi Campus,Belagavi, Karnataka, India-590008

[*]Corresponding Author : **Gujanatti Rudrappa**

Abstract **–In remote sensing applications, there exist numerous challenges in the classification of Hyperspectral images due to large amount of information processing which is required for classification, and the scarcity of labeled samples. Identifying the crops automatically is a key application in the Hyperspectral image analysis. In this article, we analyze the Support Vector Classification (SVC), Deep Neural Network (DNN) and Fusion Spectral Convolutional Neural Network (FuseNET) for crop cover classification. The results obtained for each of these methods, on standard benchmark datasets such as Indian Pines (IP), Pavia University (PU), Salinas (SA) and WHU-Hi-Longkou (WU), are presented and analyzed. The results demonstrate that FuseNET demonstrates an improvement of 13.81% for IP, 4.70% for PU, 7.13% for SA and 3.1967% for WU when compared to DNN. Also, FuseNET shows an improvement of 27.99% for IP, 18.22% for PU, 15.166% for SA and 8.02% for WU when compared to SVC.**

Keywords**—**hyperspectral imaging, crop classification, remote sensing, supervised method.

1. Introduction

An image is a 2D function A (a, b) in which ‘a’ and ‘b’ provide the spatial coordinate information and ‘a’ provides the gray level intensity information. The picture elements in the image, also termed as pixels, hold the intensity information at the coordinates (a, b) [1]. Visible light is composed of a relatively narrow band of frequencies in the electromagnetic spectrum. Colors can be represented as a set of numbers using color models to facilitate the specification of colors in some standard way, for example the RGB (Red, Green, Blue) color model.

To obtain the image data or information present within the specific wavelength ranges across the electromagnetic spectrum, Multispectral imaging technique is used which consists of less than 15 bands. To obtain much more information about the subject, hyperspectral imaging is used where hundreds of images are collected at different wavelengths, known as bands. The narrow bands of hyperspectral sensors provide a continuous spectral dimension due to which it has great potential to detect differences among various surfaces and materials [2]. Hyperspectral images (HSI) are used in many applications such as agriculture, mineralogy, food processing, surveillance, astronomy, chemical imaging and environment[3][4], so on. Crop classification will allow in knowing about their type, varieties, growing habitat and adaptability which will upgrade agricultural production [5]. Spatial and spectral information is combined because only spectral information is notenough to get the correct and accurate result [6].This paper provides a performance comparative study of the Support Vector Classification (SVC), Deep Neural network (DNN) and Fusion Spectral Convolutional Neural Network (FuseNET) methods for crop classification. Each method is used on four datasets, which are Indian Pines (IP), Pavia University (PU), Salinas Scene (SA) and WHU-Hi-Longkou (WU). Uncertainty in the spectral analysis is reduced by using FuseNET which incorporates two features viz., spectral, and spatial, for solving the limitation of spectral similarity among various crops.

Significant research has been conducted in the field of Hyperspectral imaging also known as Imaging Spectrometry in the past 40 years since the first airborne spectrometer Airborne Imaging Spectrometer (AIS) of the Jet Propulsion Laboratory (JPL) with 128 bands began its flight in 1983 [2]. Hassan et al. [5] provide an organized review on advances in agricultural technology and control strategies, briefing about various technologies applied in the agricultural domain. Zhang et al. [6] briefed the data dimension reduction techniques, classification techniques based on spectral, spatial and spectral-spatial attributes of data and available HSI datasets, highlighting the need to increase the application for cash crops. Zhonget al. [7] proposed an Iterative Support Vector Machine (ISVM) for HSI classification with automatic stopping rule and compared the performance to four Edge-Preserving filter-based (EPF-based) methods. Zhong et al. [8] proposed a “Deep Convolutional

Neural Network (D-CNN)" with Conditional Field classifier framework for accurate crop categorization using UAV Hyperspectral images and compared classification accuracies of various methods. The model showed 11.64 % improvement of overall accuracy and showed higher level generality. Lenget al. [9] presented an extensive multi feature Hyperspectral classification model which utilizes substitution of SVM at the output layer of CNN. They observed that using 4 neighboring pixels as a spatial strategy, had 3-4 % classification accuracy gain, having 8 neighboring pixels higher accuracy gain. Paolettet al. [10] provide detailed study on the state-of -the- art Deep learning (DL) methods and Machine Learning methods with experimental results of the DL methods used on the Benchmark datasets. Chao et al. [11] focus on the classification of high-dimensional and small-sample data, advantages and disadvantages of CNN over traditional classification algorithms and the relationship between the CNN Classification accuracy and the number of training samples in the case of small samples. Roy et al. [12] proposed a Hybrid model for HSI classification which has 3D-CNN facilitating both spatial and spectral feature representation from spectral bands and 2D-CNN learns more abstract level spatial representationThe comparison of Hybrid model showed it is computationally more efficient than 3D-CNN. Reshmaand Veni[13] showed that use of supervised classification for crop segmentation achieves higher accuracy than unsupervised classification methods with the combination of SVM and MNF gave an overall accuracy of 90.92 %, whereas use of ISODATA (Iterative self-Organizing Data Analysis technique) gave an overall accuracy of 50.31 %. Gorrettaet al. [14] presented a study to analyze the potential of the SWIR push broom camera to identify the "Apple scab" fungal disease by acquiring close range HSI. Bostan et al. [15] compared the accuracy of hyperspectral and multispectral images acquired through Landsat-8 and EO-1 Hyperion satellite respectively of particular agricultural fields in Turkey. The SVM classification method produced 70% and 80% accuracy for hyperspectral and multispectral images respectively. Dasiat al. [16] presented the comparison of Principle Component Analysis (PCA) and Probabilistic PCA methods. The results obtained showed that the performance is good with PCA with the Non-linear SVM and good accuracy is obtained from 20 bands from the dataset. Shamileelet al. [17] proposed the mapping of Mormon tea data acquired by the EO-1 Hyperion sensor using the Spectral Angle Mapper (SAM) classifier and ENVI software using FLAASH atmospheric correction as a necessary pre-processing step. Hu et al. [18] propose the CNN-CRF method for fine crop classification of high spatial and high spectral resolution with 91.50% accuracy with 1.00% training samples performing better than SVM and CNN.

Rest of the article is structured as follows: In **Section 2**, we list few well-known hyperspectral datasets. **Section 3** presents the general block diagram for hyperspectral image processing. In **Section 4**, we present the experimental setup. **Section 5** details the obtained results and discussion. Finally, **Section 6** concludes the study.

2. Available Datasets

Several hyperspectral sensors are available for data assembling. A list of the sensors with manufacturer and sensor features is detailed in [2]. Table 1 and Table 2 provide the information pertaining to the datasets collected by remote sensing sensors onboard the satellite and by airborne sensors made available for scientific research and study.

Table 1 List of available Hyperspectral datasets for scientific and research purposes.

S. No	Dataset	Sensor	Bands	Classes	Spatial resolution (m)	Spectral Range (um)	Image size	Time
1	Indian Pines	AVIRIS	224	16	16	0.38-2.5	145x145	1992
2	Kennedy Space center	AVIRIS	176	13	18	0.4-2.5	512x614	1996
3	Salinas	AVIRIS	224	16	3.7	0.36-2.5	512x217	1998
4	Tea Tree dataset	PHI	80	10	2.25	-	348x512	1999
5	Botswana	Hyperion	145	14	30	0.4-2.5	1476x256	2001-04
6	Pavia University	ROSIS	103	9	1.3 m	0.43-0.86	610x340	2003
7	Pavia Center	ROSIS	102	9	1.3	0.43-0.86	1096x715	2003
8	Houston	CASI 1500	144	15	2.5	-	349x1905	2012
9	WHU-Hi-HanChuan	Nano-Hyperspec	274	16	0.109	0.4-1.0	1217x303	2016
10	WHU-Hi-HongHu	Nano-Hyperspec	270	22	0.043	0.4-1.0	940x475	2017
11	WHU-Hi-LongKou	Nano-Hyperspec	270	9	0.463	0.4-1.0	550x400	2018

Table 2 Few other open-source hyperspectral images datasets.

S. No	Dataset Details	Number of Bands	Time	Reference
1.	Portion of Southern Tippecanoe County, Indiana, Aircraft scanner Flight line C1	12		
2.	2 x 2-mile portion of Northwest Tippecanoe County, Indiana, AVIRIS image Indian Pine Test Site	220	June 12, 1992	[20]
3.	AVIRIS image North-South flight line (25 x 6 mile) and East-West flight line (12 x 6 mile) portions of Northwest Tippecanoe County, Indiana)	220	June 12, 1992	[20]
4.	Hyperspectral Image: HYDICE image of Washington DC Mall	191	-	[20]
5.	The Global Hyperspectral Imaging Spectral-library of Agricultural crops (GHISA) spectral library	-	-	[21]
6.	AVIRIS Data from 2006 to present can be acquired using AVIRIS Data Products Portal	-	-	[22]
7.	Access to various land, water, crop datasets at Radiant MLHub	-	-	[23]

The information is collected as a set of 'images' by hyperspectral sensors. Each image represents the spectral band whose width is the spectral resolution of the sensor. All the captured images are combined to form a three-dimensional (a, b, λ) Hyperspectral Data cube (HDC)for processing and analysis. For the HDC a and b represent two spatial coordinates of the image and λ represents the spectral information [19].

3. Block Diagram for Hyperspectral Image Processing

Fig. 1 shows the basic steps to be carried out for hyperspectral image classification with the description as follows:

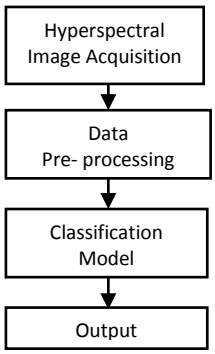

Fig. 1 Basic Steps in Hyperspectral image classification.

3.1. Hyperspectral Image Acquisition

There are four general types of spectral sensors:

(1) Whisk broom scanners (Point scanning), which acquire the spectral data for a single pixel at a time and therefore are slower,

(2) Push broom scanners (Line scanning), which acquire the spectral data of a line of pixels at a time and must have a short exposure time enough to avoid irregularity in the spectral bands,

(3) Band sequential scanners (spectral scanning), which acquire the spectral data through several images such that each image has spectral information about the x-y plane and is inconvenient for unstable environment,

(4) Snapshot hyperspectral imaging where a single shot is taken that acquires both the spatial and spectral data, but is still under development for high spatial resolution [2].

3.2. Data Preprocessing

Data pre-processing is performed for improving the image data, cracking down unwanted distortion which helps in further processing. Pre-processing includes -

(1) Image enhancement

(2) Colour conversion

(3) Resizing and filtering of images

(4) Quality estimation of hyperspectral images, which is characterized by Signal to Noise ratio (SNR) [1].

(5) Data dimensionality reduction and Feature Extraction: Using PCA, Minimum Noise Fractional Transform (MNF) and Linear Discriminant Analysis (LDA) for optimal band selection to reduce data dimensionality and for removal of radiometric noise [13].

3.3. Classification

Classification assigns a label to an object based on its descriptors [1]. Once the hyperspectral data cubes are reduced dimensionally using the data reduction techniques, sample recognition can then be performed using either supervised or unsupervised classification techniques [6]. Professionals not needed to enter into details of image processing and classification may use the Software and Libraries available to deal with Hyperspectral Data as briefed in [2].

4. Experiment Setup

In this section, we detail the experiment setup. Fig. 2 shows the flow diagram of proposed methodology for the classification of the HSI datasets**.**

4.1. Dataset Description

We have used four publicly available hyperspectral image datasets, namely Indian Pines, University of Pavia and Salinas Scene and WHU-Hi-LongKou dataset . The details of these datasets are present in Table 1.

4.2. Feature Extraction Technique-Principal Component Analysis

PCA is an unsupervised learning algorithm that is used for dimensionality reduction, feature extraction, spectral denoising and data denoising in machine learning algorithms. PCA Algorithm for feature extraction as presented in [24]:

(1) Standardizing or normalizing the datasets.
(2) Creation of Covariance matrix.
(3) Perform Decomposition of Covariance matrices into Eigenvectors.
(4) Selection of important Eigenvectors.
(5) Creation of projection matrix using k eigenvectors.
(6) Transform input image to new feature space using projection matrix.

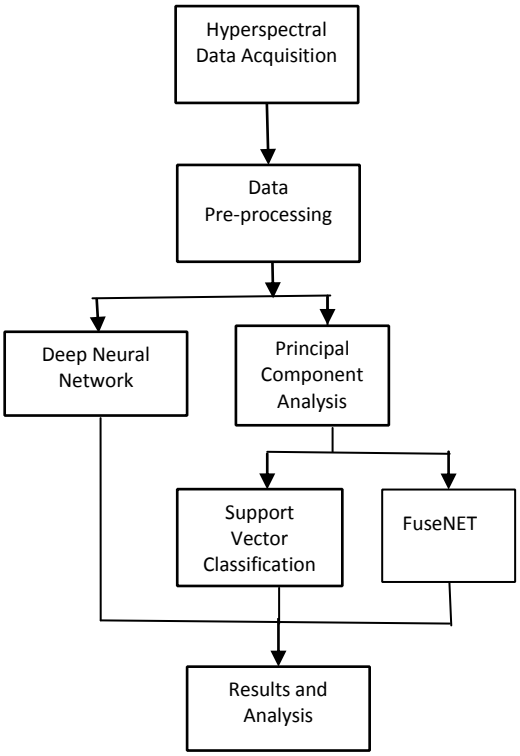

Fig. 2 Flow diagram of proposed methodology for crop classification.

4.3. Classification

We study the DNN, SVC and FuseNET methods to classify the values in the different datasets.

(1) Deep Neural Networks: DNN is a feedforward, Artificial Neural Network (ANN) with additional depth. DNN deals with unlabeled or unstructured data. We are using DNN with 12 Fully connected layers, Batch normalization (for faster convergence) and dropout layers. The DNN has Rectified Linear Unit (ReLU) as the activation function. For training computationally efficient Adam optimizer, Categorical cross-entropy, accuracy as metric and callback is used.

(2) Support Vector Classification: Support Vector Machine for supervised classification is detailed in [25]. The extracted spectral features are then treated with non-linear radial basis function kernel-based SVM Classifiers. Here the datasets are passed through the Principal Component Analysis kernel. Multiple class support is handled with SVC according to one versus one scheme. PCA is applied to reduce the number of spectral bands.

(3) Fusion Spectral Convolutional Neural Network: FuseNET stacks both 3D-CNN and 2D-CNN layers to utilize both the spectral as well as spatial feature maps to their full extent to achieve maximum possible accuracy. Only using 2D CNN fails to consider spectral information. Using only 3D CNN exploits both spectral-spatial information, but comes at the expense of increased computational complexity. PCA is used to reduce spectral bands. In this method, the window of size 25 is used to create image cubes to feed into the model. Prior to image cube creation, padding with zeros is done. Adam optimizer is used with learning rate of 0.001, accuracy as metric and early stopping checkpoint is used. The model is validated on test images.

5. Results and Discussion

In this section we present the obtained results and related discussions. Tables 3–6 present detailed classification reports obtained for Indian Pines (IP), Pavia University, Salinas scene and Wuhan-Hi-LongKoudatasets for each of the specified methods for a test ratio of 0.3. Note that in all of the tables below, ‘P’,’R’ and ‘F1-S’ represent the Precision, Recall and F1-score respectively. Precision denotes the fraction of predictions made as positive class are actually positive. Recall also known as True Positive Rate (TPR) denotes the fraction of all positive samples that were correctly predicted as positive. F1-Score is the harmonic mean of precision and recall. Class samples for IP, SA and PU are available in [26] and for WU in [8].

As seen from Table 3, the P, R and F1-score values for IP using DNN are 0 for Class 7, because the samples for Class 7 are among the lowest or 0 as compared to remaining classes. Also, this is probably due to the presence of two classes (namely Grapes-pastures and Grass-trees) which have very similar textures over most spectral bands. Using the SVC method for IP, PU and SA datasets showed that the P, R and F1-score values for some classes are either zero or very small. This is because the number of samples of those classes is comparatively very less than that of other classes or likely there are identical classes. SVC however works well on the WU dataset. This is because the number of class samples is higher compared to that of other datasets.

The FuseNET method performs well and gives highest P, R and F1-score values for most of the classes in all four datasets compared to the other three methods. The 3D-CNN and 2D-CNN layers assembled in FuseNET utilize both the spectral as well as spatial feature maps to their full extent to achieve maximum possible accuracy. FuseNET outperforms other methods, showing minimum deviation. By increasing the window size for the FuseNET model from 19 to 21, we observed a decrease in performance by 0.01% for IP, 0.08% for PU and 0.300% for SA. On further increasing size to 25, we see a rise of 1.000% for IP, 0.000% for PU and 0.010% for SA.

Table 3 Classification performance for Indian Pines dataset.

Class No.	**Class Name**	**DNN**			**FuseNET**			**SVC**		
		P	R	F1-S	P	R	F1-S	P	R	F1-S
1	Alfalfa	86	55	67	100	100	100	00	00	00
2	Corn-notill	85	79	82	100	100	100	59	53	56
3	Corn-mintill	68	86	76	100	94	97	83	25	38
4	Corn	75	65	69	100	100	100	100	13	24
5	Grass-pastures	96	94	95	94	100	97	96	58	72
6	Grass-trees	99	91	95	100	100	100	88	63	74
7	Grass-pastures-mowed	00	00	00	100	100	100	00	00	00
8	Hay-windrowed	99	98	98	100	100	100	77	100	87
9	Oats	67	80	73	100	100	100	00	00	00
10	Soybean-notill	91	83	86	99	100	100	67	65	66
11	Soybean-mintill	83	88	85	100	100	100	59	82	69
12	Soybean-clean	88	79	83	100	95	95	71	27	39
13	Wheat	98	94	96	79	100	100	86	86	86
14	Woods	98	91	94	100	100	100	75	25	38
15	Buildings-Grass-Trees-Drives	49	85	62	100	100	100	00	00	00
16	Stone-Steel-Towers	93	93	93	86	100	100	81	81	81
17	No class	-	-	-	-	-	-	75	90	82

The results obtained for IP dataset is shown in Fig. 3, in which Fig. 3(a) shows the Ground Truth image of the dataset. Figs. 3(b)-(c) show the predicted classification map by using FuseNET, DNN and SVC methods respectively. The quality of classification maps of FuseNET is far better than other methods, also at the smaller regions in the map. Similarly, classification maps for SA, PU and WU datasets are presented in Figs. 4, 5 and 6 respectively.

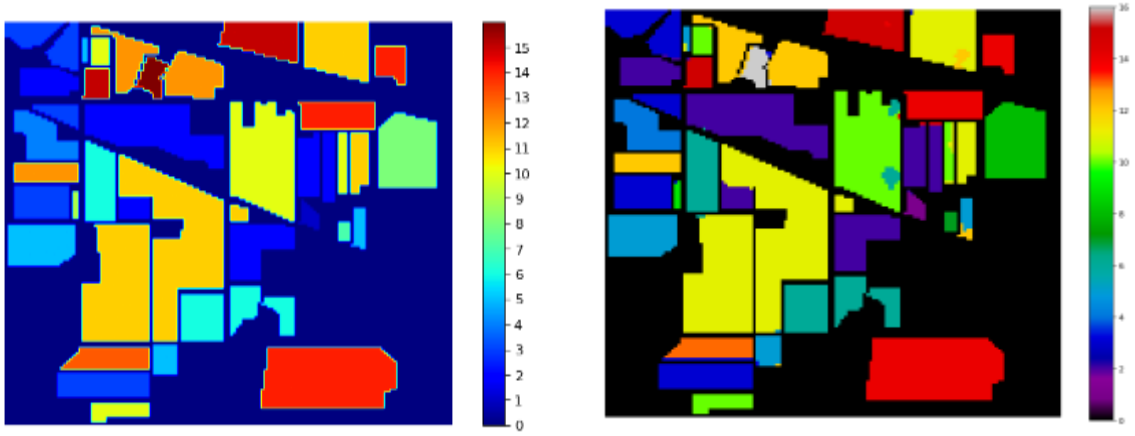

(a) Ground truth image.

(b) Predicted classification maps for FuseNET

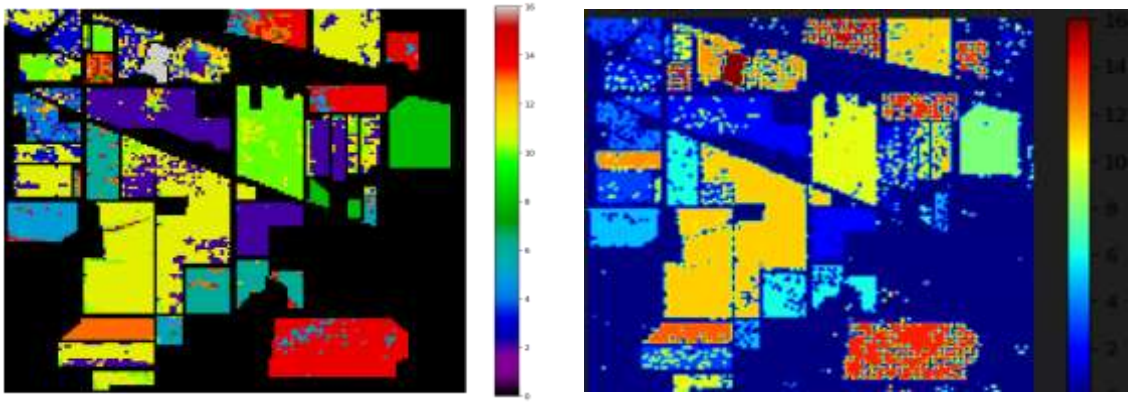

(c) Predicted classification maps for DNN

(d) Predicted classification map for SVC

Fig. 3 Classification map for IP.

Table 4 Classification performance for Salinas Scene dataset.

Class No.	Class Name	DNN			FuseNET			SVC		
		P	R	F1-S	P	R	F1-S	P	R	F1-S
1	Brocoli_green_weeds_1	100	99	99	100	100	100	82	98	89
2	Brocoli_green_weeds_2	99	100	100	100	100	100	84	99	91
3	Fallow	100	93	93	100	100	100	00	00	00
4	Fallow_rough_plow	100	99	99	100	100	100	80	75	77
5	Fallow smooth	96	99	99	100	100	100	77	95	85
6	Stubble	100	100	100	100	100	100	87	98	92
7	Celery	100	100	100	100	100	100	89	99	94

8	Grapes untrained	91	80	80	100	100	100	72	91	80
9	Soil vineyard develop	100	99	99	100	100	100	85	88	87
10	Corn senesced green weeds	93	98	98	100	100	100	81	81	81
11	Lettuce romaine 4wk	97	96	96	100	100	100	00	00	00
12	Lettuce romaine 5wk	100	98	98	100	100	100	83	74	78
13	Lettuce romaine 6wk	100	99	99	100	100	100	69	98	81
14	Lettuce_romaine_7wk	97	98	98	100	100	100	71	83	77
15	Vineyard untrained	66	84	84	100	100	100	80	49	61
16	Vineyard vertical trellis	99	100	100	99	100	100	93	95	94
17	No class	-	-	-	-	-	-	89	89	89

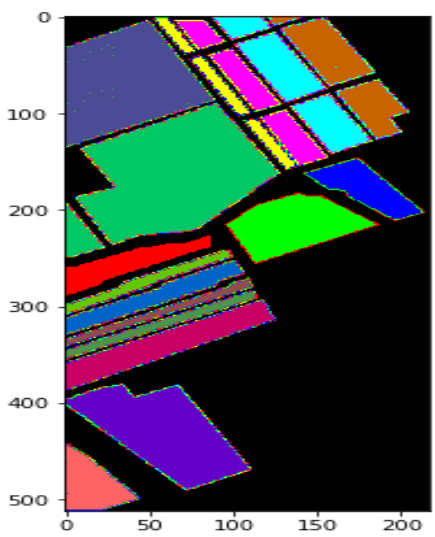

(a) Ground truth image

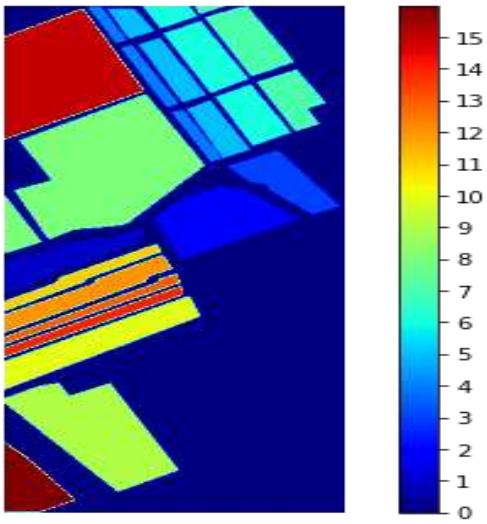

(b) Predicted classification maps for FuseNET

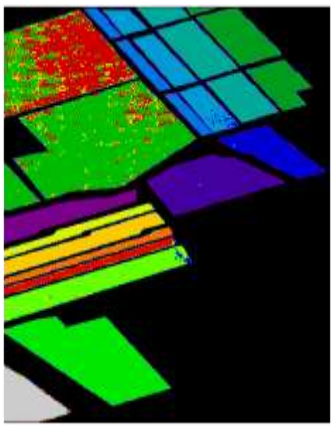

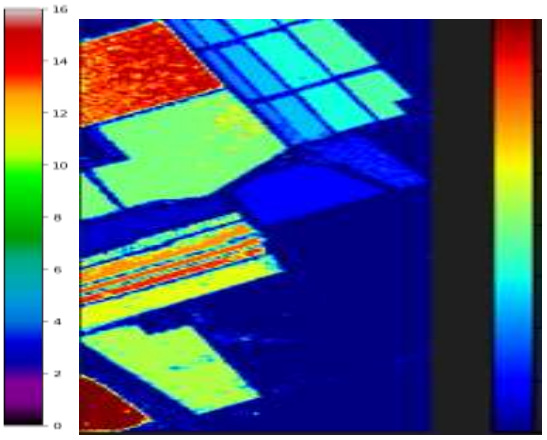

(c) Predicted classification maps for DNN

(d) Predicted classification maps for SVC

Fig. 4 Classification map for SA.

Table 5 Classification performance for Pavia University dataset.

Class No.	Class Name	DNN			FuseNET			SVC		
		P#	R	F1-S	P	R	F1-S	P	R	F1-S
1	Asphalt	93	97	95	98	100	99	00	00	00
2	Meadows	99	97	98	100	100	100	76	24	37
3	Gravel	75	84	79	100	97	98	00	00	00
4	Trees	93	96	95	100	100	100	00	00	00
5	Painted metal sheets	100	100	100	100	100	100	77	94	85
6	Bare soil	94	95	95	100	100	100	00	00	00
7	Bitumen	90	84	87	95	100	97	00	00	00
8	Self- blocking Bricks	90	83	86	99	96	97	00	00	00
9	Shadows	100	100	100	100	99	99	00	00	00
10	No class	-	-	-	-	-	-	81	99	89

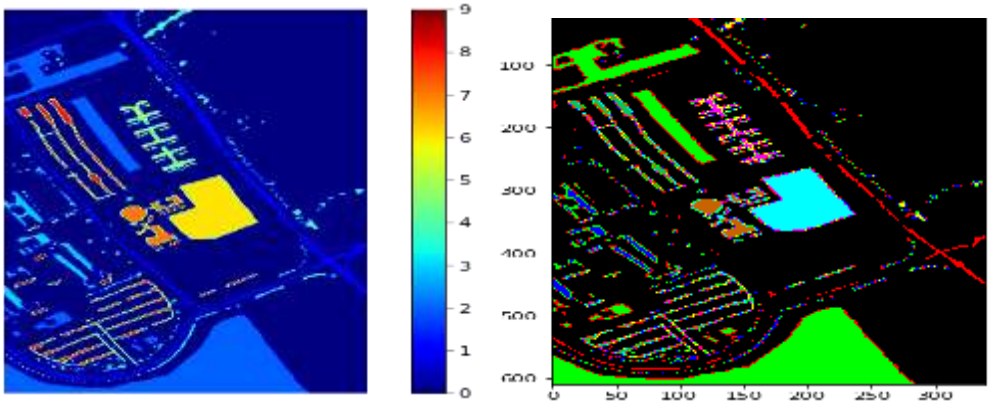

(a) Ground truth image

(b) Predicted classification maps for FuseNET

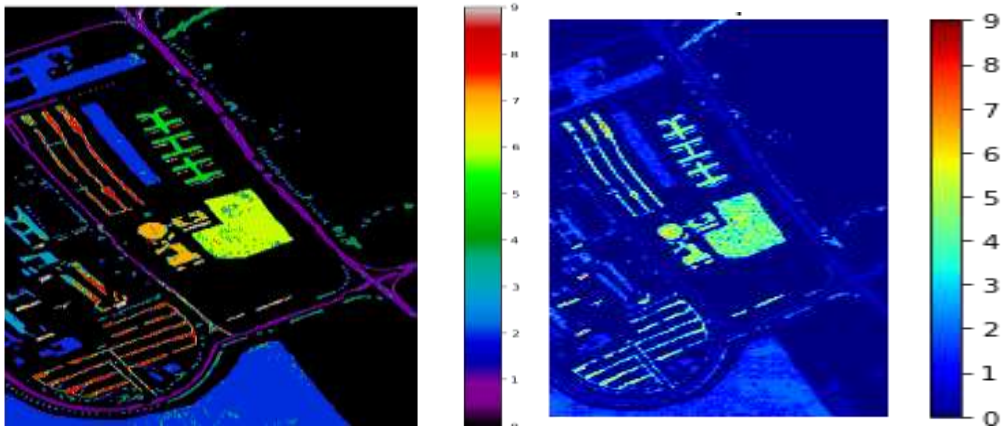

(c) Predicted classification maps for DNN

(d) Predicted classification maps for SVC

Fig. 5.Classification map for PU.

Table 6 Classification performance for WHU-Hi-LongKou dataset.

Class No.	Class Name	DNN			FuseNET			SVC		
		P	R	F1-S	P	R	F1-S	P	R	F1-S
1	Corn	99	100	100	100	100	100	94	98	96
2	Cotton	75	72	74	99	100	100	81	82	81
3	Sesame	92	98	95	100	100	100	95	67	79
4	Broad leaf soyabean	98	98	98	100	100	100	89	98	93
5	Narrow leaf soyabean	62	52	57	100	99	99	76	54	63
6	Rice	99	100	100	100	100	100	92	99	95
7	Water	100	100	100	100	100	100	99	100	99
8	Roads and houses	84	90	87	98	99	99	82	87	84
9	Mixed Weeds	96	95	96	99	98	99	90	59	71
10	No class	-	-	-	-	-	-	74	47	58

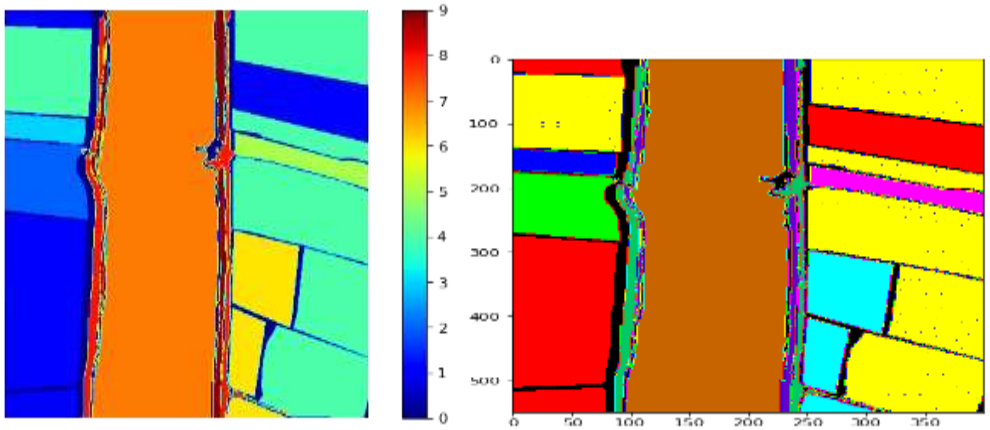

(a) Ground truth image

(b) Predicted classification maps for FuseNET

(c) Predicted classification maps for DNN

(d) Predicted classification maps for SVC

Fig. 6 Classification map for WU.

Table 7 represents the results in terms of Average Accuracy (AA), Overall Accuracy (OA) and Kappa Coefficient (KC) for the DNN, SVC and FuseNET methods.

Cohen's kappa i.e., Kappa coefficient takes imbalance in class distribution into account and can, therefore, be more complex to interpret [27]. Overall accuracy is the ratio of the number of correct predictions and the total number of predictions. The AA, OA, KC values are calculated using the formulae from [28]. FuseNET outperforms other methods by being efficient even for 30% training and 70% testing samples. Using FuseNET and 0.70% as test ratio, an accuracy of 96.19%, 95%,98.74% and 97.00% was obtained for IP, PU, SA and WU. This shows that FuseNET retained its performance in accuracy representing high discriminative features even with increase in window size (Use of 25*25 as spatial dimension is more suitable) training set comprising only 30% and is also computationally efficient in terms of Train-test timing.

Table 7 The classification accuracies (in percentages) on Indian Pines, Pavia University, Salinas Scene and WHU-Hi-LongKou datasets.

Method	Indian Pines			Pavia University			Salinas scene			WHU-Hi-Longkou		
	OA	KC	AA	OA	KC	AA	OA	KC	AA	OA	KC	AA
DNN	86.01	73.76	84.09	94.70	92.10	93.10	92.83	91.11	96.63	96.60	94.80	89.60
SVC	71.86	56.06	43.91	81.27	20.83	21.66	84.80	77.77	77.07	91.78	88.60	78.94
FuseNET	99.80	98.86	99.30	99.38	98.68	98.61	99.96	98.88	99.93	99.79	98	99.51

6. Conclusion

In this paper, we have classified the crops using different machine learning approaches. Datasets are used to test the effectiveness of various Hyperspectral classification methods. It is observed from the obtained results that the overall accuracy, Kappa coefficient and Average Accuracy is improved significantly by using the FuseNET model. Further, FuseNET is effective due to the capacity to extract highly discriminatory features and effectively leverage the spatial-contextual and spectral information contained in HSI data cubes. The model also shows an excellent performance for small training data.

We also observed from the results that due to spectral similarity among different crops, noise exists and there is misclassification. The model, considering the spatial neighborhood information (DNN and FuseNET) shows better visual performance compared to SVC. DNN, using only local spatial information, results in the local optima during training, providing detached misclassification results in classification map. Exploiting both, spatial-spectral features, FuseNET performs better in comparison to SVC and DNN.

References

[1] R. C. Gonzalez and R. E. Woods, Digital Image Processing, 4th ed., Upper Saddle River, NJ, USA: Prentice-Hall, Inc., 2018.

[2] T. Adao, J. Hruška, L. Pádua, J. Bessa, E. Peres, R. Morais, and J. Sousa, "Hyperspectral Imaging: A Review on UAV-Based Sensors, Data Processing and Applications for Agriculture and Forestry," Remote Sensing, vol. 9, no. 11, p. 1110, October 2017.

[3] G. Rudrappa, A. A. Shetty, A. G. Kulkarni, A. R. Jujagaon, N. Vijapur, and A. D. Khelgi, "Pixel Saturation Applied for Cloud Cover Estimation in Ground based All Sky Images," J. Pharm. Negat. Results, vol. 13, no. 3, pp. 173–176, 2022, doi: 10.47750/pnr.2022.13.S03.029.

[4] G. Rudrappa, V. Nataraj, J. Sushant, and M. Prabhakar, "Cloud Classification Using Ground Based Images Using CBIR and K-Means Clustering," Biosci. Biotechnol. Res. Commun., vol. 13, no. 13, pp. 95–99, 2020, doi: 10.21786/bbrc/13.13/13.

[5] S. I. Hassan, M. M. Alam, U. Illahi, M. A. Al Ghamdi, S. H. Almotiri and M. M. Su'ud, "A Systematic Review on Monitoring and Advanced Control Strategies in Smart Agriculture," IEEE Access, vol. 9, pp. 32517-32548, February 2021.

[6] Y. Zhang, D. Wang and Q. Zhou, "Advances in crop fine classification based on Hyperspectral Remote Sensing," 8th International Conference on Agro-Geoinformatics (Agro-Geoinformatics), pp. 1-6, 2019.

[7] S. Zhong, C. -I. Chang and Y. Zhang, "Iterative Support Vector Machine for Hyperspectral Image Classification," 25th IEEE International Conference on Image Processing (ICIP), pp. 3309-3312, 2018.

[8] Y. Zhong, X. Hu, C. Luo, X. Wang, J. Zhao, L. Zhang, "WHU-Hi: UAV-borne hyperspectral with high spatial resolution (H2) benchmark datasets and classifier for precise crop identification based on deep convolutional neural network with CRF", Remote Sensing of Environment, Volume 250, 112012, 2020.

[9] J. Leng, T. Li, G. Bai, Q. Dong and H. Dong, "Cube-CNN-SVM: A Novel Hyperspectral Image Classification Method," IEEE 28th International Conference on Tools with Artificial Intelligence (ICTAI), pp. 1027-1034, 2016.

[10] M. E. Paoletti, J.M. Haut, J. Plaza, A. Plaza, "Deep learning classifiers for hyperspectral imaging: A review", ISPRS Journal of Photogrammetry and Remote Sensing, Volume 158, pp. 279-317, 2019.

[11] M. Chao and G. Meng-Yuan, "Hyperspectral Image Classification Based on Convolutional Neural Network," 5th International Conference on Information, Cybernetics, and Computational Social Systems (ICCSS), pp. 117-121, 2018.

[12] S. K. Roy, G. Krishna, S. R. Dubey and B. B. Chaudhuri, "HybridSN: Exploring 3-D–2-D CNN Feature Hierarchy for Hyperspectral Image Classification," IEEE Geoscience and Remote Sensing Letters, vol. 17, no. 2, pp. 277-281, Feb. 2020.

[13] S. Reshma and S. Veni, "Comparative analysis of classification techniques for crop classification using airborne hyperspectral data," International Conference on Wireless Communications, Signal Processing and Networking (WiSPNET), pp. 2272-2276, 2017.

[14] N. Gorretta, M. Nouri, A. Herrero, A. Gowen and J. Roger, "Early detection of the fungal disease "apple scab" using SWIR hyperspectral imaging," 10th Workshop on Hyperspectral Imaging and Signal Processing: Evolution in Remote Sensing (WHISPERS), pp. 1-4, 2019.

[15] S. Bostan, M. A. Ortak, C. Tuna, A. Akoguz, E. Sertel and B. Berk Ustundag, "Comparison of classification accuracy of co-located hyperspectral & multispectral images for agricultural purposes," Fifth International Conference on Agro-Geoinformatics (Agro-Geoinformatics), pp. 1-4, 2016.

[16] S. Dasi, D. Peeka, R. B. Mohammed and B. L. N. Phaneendra Kumar, "Hyperspectral Image Classification using Machine Learning Approaches," 2020 4th International Conference on Intelligent Computing and Control Systems (ICICCS), pp. 444-448, 2020.

[17] H. Shamileel, J. V. Balaji, S. Praveen and J. Aravinth, "Mapping of Mormon Tea Species using Hyperion Hyperspectral Data," International Conference on Wireless Communications Signal Processing and Networking (WiSPNET), pp. 180-185, 2019.

[18] X. Hu, Y. Zhong, C. Luo and L. Wei, "Fine Classification of Typical Farms in Southern China Based on Airborne Hyperspectral Remote Sensing Images," 7th International Conference on Agro-geoinformatics (Agro-geoinformatics), pp. 1-4, 2018.

[19] M. J. Khan, H. S. Khan, A. Yousaf, K. Khurshid and A. Abbas, "Modern Trends in Hyperspectral Image Analysis: A Review," in IEEE Access, vol. 6, pp. 14118-14129, 2018.

[20] Purdue Engineering, "MultiSpec© | Tutorials," Purdue Research Foundation. Available: https://engineering.purdue.edu/~biehl/MultiSpec/hyperspectral.html . [Accessed: January 14, 2022]

[21] CMR Research, "Global Hyperspectral Imaging Spectral-library of Agricultural crops for Central Asia V001", Available: https://cmr.earthdata.nasa.gov/search/concepts/C1704836117-LPDAAC_ECS.html. [Accessed: January 15, 2022]

[22] AVIRIS - Airborne Visible / Infrared Imaging Spectrometer - Data, "AVIRIS - Airborne Visible / Infrared Imaging Spectrometer - Data", September 17, 2020. [Online]. Available: https://aviris.jpl.nasa.gov/data/get_aviris_data.html.[Accessed: January 15, 2022]

[23] Radiant MLHub- Earth Imagery for Impact [Online]. Available: https://mlhub.earth/ [Accessed: June 19, 2022]

[24] Fernandez D., Gonzalez, C., Mozos, D. et al., "FPGA implementation of the principal component analysis algorithm for dimensionality reduction of hyperspectral images," J Real-Time Image Proc 16, 1395–1406 (2019). https://doi.org/10.1007/s11554-016-0650-7.

[25] M. Awad, R. Khanna, “Support Vector Machines for Classification," in Efficient Learning Machines. Apress, Berkeley, CA, 2015, pp-39-66. Available: https://doi.org/10.1007/978-1-4302-5990-9_3.

[26] M Graña, MA Veganzons and B Ayerdi , “Hyperspectral Remote Sensing Scenes,”, July 2021. Available: https://www.ehu.eus/ccwintco/index.php/Hyperspectral_Remote_Sensing_Scenes . [Accessed: 19 June, 2022]

[27] MaaritWidmann, “Cohen’s Kappa: What It Is, When to Use It, and How to Avoid Its Pitfalls”, Aug. 20, 2020. [Online]. Available: https://thenewstack.io/cohens-kappa-what-it-is-when-to-use-it-and-how-to-avoid-its-pitfalls/ [Accessed: 19 June, 2022]

[28] J. Mohajon, “Confusion Matrix for Your Multi-Class Machine Learning Model”, May 29, 2020. Available: https://towardsdatascience.com/confusion-matrix-for-your-multi-class-machine-learning-model-ff9aa3bf7826, [Accessed: June 19, 2022]